Kinetics of Insulin-Mediated and Non–Insulin-Mediated Glucose Uptake in Humans

STEVEN V. EDELMAN, MARKKU LAAKSO, PENNY WALLACE, GINGER BRECHTEL, JERROLD M. OLEFSKY, AND ALAIN D. BARON

The kinetics of insulin-mediated glucose uptake (IMGU) and non–insulin-mediated glucose uptake (NIMGU) in humans have not been well defined. We used the glucose-clamp technique to measure rates of whole-body and leg muscle glucose uptake in six healthy lean men during hyperinsulinemia (~460 pM) to study IMGU and during somatostatin-induced insulinopenia to study NIMGU at four glucose levels (4.5, 9, 12, and 21 mM). To measure leg glucose uptake, the femoral artery and vein were catheterized, and blood flow was measured by thermodilution (leg glucose uptake = arteriovenous glucose difference [A-V_G] × blood flow). With this approach, we found that, during hyperinsulinemia, both whole-body and leg glucose uptake increased in a curvilinear fashion at every glucose level, the highest glucose uptake values obtained being 139 ± 17 μmol · kg^{-1} · min^{-1} and 3656 ± 931 μmol · min^{-1} · leg^{-1}, respectively. Leg blood flow increased twofold from 6.0 ± 1.7 to 11.7 ± 3.1 dl/min ($P < 0.01$) over the range of glucose and was correlated with whole-body glucose uptake ($r = 0.55$, $P < 0.005$). Leg muscle glucose extraction, independent of changes in blood flow, which is reflected by the A-V_G, saturated over the range of glucose (1.28 ± 0.12, 2.22 ± 0.30, 2.92 ± 0.42, 3.02 ± 0.41 mM, NS between last 2 values) with a half-maximal effective glucose concentration (EG_{50}) of 5.3 ± 0.4 mM. During insulinopenia, both whole-body and leg glucose uptake increased in a near-linear fashion; however, glucose uptake remained significantly lower than that seen with insulin stimulation, the highest glucose uptake values obtained being 22 ± 2 μmol · kg^{-1} · min^{-1} and 260 ± 34 μmol · min^{-1} · leg^{-1}, respectively. Leg blood flow was unchanged from the basal value (4.15 ± 0.63 dl/min) over the range of glucose studied, and A-V_G increased at all glucose levels: 0.094 ± 0.010, 0.28 ± 0.03, 0.38 ± 0.04, and 0.59 ± 0.03 mM ($P < 0.05$ between any 2 consecutive values), with an EG_{50} of 10.0 ± 0.4 mM ($P < 0.001$ vs. IMGU). We conclude that *1)* insulin increases the capacity for muscle A-V_G approximately fivefold; *2)* muscle IMGU, independent of blood flow, displays an EG_{50} similar to the K_m characteristic of the glucose-transport system (~5–6 mM); *3)* in contrast, NIMGU is a low-affinity glucose-uptake system; and *4)* blood flow to insulin-sensitive tissue increases with insulin and glucose infusions and is an important determinant of the rate of in vivo glucose uptake. *Diabetes* 39:955–64, 1990

From the Department of Medicine, Veterans Administration Medical Center, Research Service, San Diego and Indianapolis; the University of California, San Diego, California; and the Indiana University Medical Center, Indianapolis, Indiana.

Address correspondence and reprint requests to Alain D. Baron, MD, Indiana University School of Medicine, 545 Barnhill Drive, Emerson Hall 421, Indianapolis, IN 46202-5124.

Received for publication 5 December 1988 and accepted in revised form 6 April 1990.

One of the major in vivo effects of insulin is to stimulate overall glucose disposal. This is accomplished by a marked 5- to 10-fold increase in overall whole-body glucose disposal rates (1–3). However, the mechanisms underlying this effect are poorly understood. For example, it is not known whether insulin increases the V_{max} of glucose disposal, decreases the K_m, or both. In vitro studies of insulin's effect on glucose uptake have largely focused on the glucose-transport step. Thus, several studies have shown that insulin leads to an increase in V_{max} with no change in K_m of glucose transport in adipose (4–9) and muscle (10–12) tissues. However, more recent studies have shown that, in addition to increasing V_{max}, insulin also lowers the K_m for glucose transport (13–16). Whether these in vitro data can be directly extrapolated to the intact in vivo situation is unclear.

Gottesman et al. (17) reported that insulin stimulates whole-body glucose uptake by increasing V_{max} without a change in the K_m for glucose uptake. However, glucose uptake was studied over a relatively narrow range of serum glucose concentrations (3.3–8.9 mM), over which saturation of the glucose-uptake system was not approached. Yki-Järvinen et al. (18) measured rates of glucose uptake over a wide range of glucose and insulin concentrations in the

whole body and across forearm muscle. At low insulin levels (65 pM), they reported that glucose uptake follows Michaelis-Menten kinetics with a K_m characteristic of the glucose-transport system (~5–6 mM). However, at higher insulin concentrations (>356 pM), they reported an increase in both V_{max} and K_m and interpreted these data to represent a change in the rate-limiting step for glucose uptake from transport at low insulin concentrations to a step distal to the glucose-transport system at higher insulin concentrations. These in vivo data are conflicting in part because in vivo studies of the kinetics of whole-body glucose uptake represent the net contribution of several tissues, only some of which are insulin sensitive. Glucose uptake occurs via two mechanisms: insulin-mediated glucose uptake (IMGU), which occurs only in insulin-sensitive tissues (i.e., muscle and adipocytes), and non–insulin-mediated glucose uptake (NIMGU), which occurs in both insulin-sensitive and non–insulin-sensitive tissues (i.e., brain, blood cells, nerve, etc.). Previous data from our laboratory indicate that NIMGU and IMGU are separately regulated and functionally distinct glucose-uptake systems (19,20). In the light of these data, we reasoned that these two glucose-uptake systems might also display different kinetic characteristics.

This study was designed to examine insulin's effect on the capacity and affinity of the in vivo glucose-uptake system. Using in part the data presented in this article, we previously reported that in vivo IMGU is largely accounted for by skeletal muscle (21). Therefore, we addressed this issue by assessing the kinetic parameters of glucose uptake (V_{max} and K_m) in the whole body and across leg muscle in six lean healthy men. Studies were done over a wide range of serum glucose concentrations with the glucose-clamp technique combined with femoral arterial and venous catheterization. Measurements were performed during a 40-mU · m^{-2} · min^{-1} insulin infusion to assess the kinetics of IMGU and during somatostatin (SRIF)-induced insulinopenia to assess the kinetics of NIMGU.

RESEARCH DESIGN AND METHODS

Pork monocomponent insulin was generously supplied by Lilly (Indianapolis, IN); ^{125}I-labeled insulin and [3-^{3}H]glucose (sp act 13.5 Ci/nmol) were purchased from Du Pont-NEN (Boston, MA); bovine serum albumin (fraction V) was obtained from Armour (Chicago, IL); guinea pig anti-insulin antibody was kindly supplied by E. Arquilla (Univ. of California, Irvine, CA); and SRIF (cyclic form) was purchased from Bachem (Torrance, CA).

The study group for studies 1 and 2 consisted of six healthy nonobese men; study 3 consisted of five healthy nonobese men. All had a normal oral glucose tolerance test (75-g glucose load) as defined by the criteria of the National Diabetes Data Group (22). The combined mean ± SD age and weight of the groups for studies 1 and 2 were 31.5 ± 6.1 yr and 68.6 ± 3.9 kg and for study 3 were 36.2 ± 5.2 yr and 69.1 ± 4.3 kg. All subjects were admitted to the Veterans Administration Medical Center Special Diagnostic and Treatment Unit (La Jolla, CA). While hospitalized, they remained active to approximate their prehospital exercise level. All subjects were chemically euthyroid and normotensive, and no subject had a concurrent disease or was ingesting pharmacological agents known to affect carbohydrate or insulin metabolism or the cardiovascular system. Studies were approved by the Human Subjects Research Review Committee, and all subjects gave written informed consent.

All subjects were fed a weight-maintenance diet (~32 cal · kg^{-1} body wt · day^{-1}), with three divided feedings containing 20, 40, and 40% of the total daily calories given at 0800, 1200, and 1700, respectively. The calorie content of the diet was 50% carbohydrate, 20% fat, and 30% protein. All subjects ate this diet for at least 48 h before any studies were performed.

Details of the study protocol are shown in Fig. 1. Each subject underwent two randomly sequenced studies, each performed ~1 mo apart after an overnight fast. Study 1 was designed to measure basal whole-body glucose turnover with [3-^{3}H]glucose and basal leg glucose uptake (arteriovenous femoral catheterization technique). In addition, whole-body and leg NIMGU were measured at euglycemia and over a wide range of glucose concentrations to characterize the K_m and V_{max} of NIMGU. Glucose-turnover data measured at basal and the first and third glycemic plateaus in these subjects have been previously published (21). To measure turnover, [3-^{3}H]glucose was infused through a catheter placed into an antecubital vein starting at 0630. At ~0800, catheters were inserted into the right femoral artery and vein (see technique below). At least 40 min after the femoral catheters were inserted, arterial blood was obtained at 5-min intervals over 20 min to determine basal serum glucose; plasma glucose specific activity; and serum insulin, C-peptide, epinephrine, and free–fatty acid (FFA) levels. Simultaneously, femoral venous blood was obtained to determine serum glucose levels. Basal leg blood flow was also determined (see technique below). After the basal measurements were obtained, an infusion of SRIF (0.16 μg · kg^{-1} · min^{-1}) was started at time 0 to suppress endogenous insulin

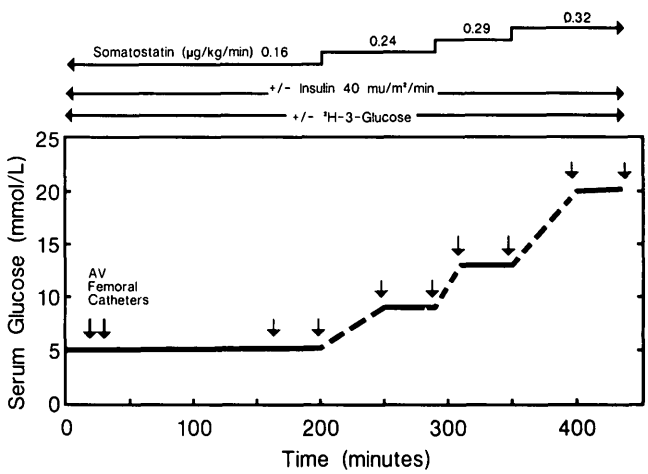

FIG. 1. Study design. On separate days, non–insulin-mediated glucose uptake (somatostatin, no insulin replacement, and [3-^{3}H]glucose) and insulin-mediated glucose uptake (somatostatin and insulin replacement) were measured in 6 subjects at 4 sequential glucose plateaus (~5, 9, 12, 21 mM, *solid lines*) in whole body and in leg with glucose-clamp and limb-balance techniques. *Arrows* indicate when blood for hormone and metabolic data were collected and when leg blood-flow measurements were made. *Dashed lines* represent time interval necessary to raise serum glucose level to next glycemic plateau. Somatostatin was infused in stepwise fashion to inhibit breakthrough of endogenous insulin secretion (see text for details). AV, arteriovenous.

secretion, and the arterial serum glucose level was held at the basal level with the glucose-clamp technique. Because the biological effect of insulin to stimulate glucose-uptake decays with an apparent half-time of 40 min (23), it follows that, after 120 min of severe SRIF-induced insulinopenia, isotopically determined glucose uptake and leg glucose uptake represent NIMGU. Therefore, NIMGU at euglycemia (4.9 mM) was measured after 120 min of SRIF infusion. Subsequently, the glucose level was raised and clamped at three additional plateaus (9.2, 11.9, and 20.5 mM). Each glucose plateau period lasted ~40 min. The SRIF infusion rate was increased to 0.24, 0.29, and 0.32 $\mu g \cdot kg^{-1} \cdot min^{-1}$ at the respective glucose plateaus to prevent breakthrough of endogenous insulin secretion. During each plateau period, leg balance was determined as previously described (21).

Study 2 was designed to assess the kinetics of whole-body and leg IMGU. To accomplish this, insulin (40 $mU \cdot m^{-2} \cdot min^{-1}$) was infused to achieve physiological hyperinsulinemia (~460 pM) starting at 0700 through a catheter inserted into an antecubital vein. The serum glucose level was clamped at the basal value by use of arterialized venous blood obtained from a catheter inserted retrogradely into a distal dorsal hand vein and the hand placed in a warming device until the femoral catheters were inserted (~0800), at which time the arterial serum glucose concentration was clamped, and the hand catheter was removed. All subjects achieved steady-state insulin action after 160 min of insulin infusion (24). Therefore, glucose-turnover data were obtained from 160 to 200 min at euglycemia (4.5 mM) and over 40 min at glucose plateaus of 8.7, 12.1, and 21.0 mM, respectively. Glucose-turnover data obtained at the first and third glycemic plateaus in these subjects have been previously published (21). In this condition, infusion of [3-^{3}H]glucose was not necessary, because hepatic glucose production is completely suppressed during the combination of hyperinsulinemia and SRIF-induced glucagon deficiency (25). Thus, the whole-body glucose disposal rate was taken as the exogenous glucose infusion rate corrected for the change in glucose mass in a distribution volume of 19% body weight. Rates of IMGU were calculated as the difference between the insulin-stimulated glucose disposal rate (GDR) and the rate of NIMGU measured at the same serum glucose level; i.e., IMGU = GDR − NIMGU. Leg glucose uptake was estimated by the leg-balance technique (21).

Because it is possible that the rates of glucose uptake obtained during the stepped glycemic protocol used in this study could be different than if the rates of glucose uptake were obtained during clamps performed at a single glucose level on separate days, we performed the following separate studies to validate our protocol. In study 3, we performed paired glucose-clamp studies in five lean subjects (not studied in study 1 or 2) during the coinfusion of SRIF (0.16 $\mu g \cdot kg^{-1} \cdot min^{-1}$) and insulin (120 $mU \cdot m^{-2} \cdot min^{-1}$). The glucose-clamp studies differed such that one was carried out at hyperglycemia (14.7 ± 0.4 mM) over 5 h (nonstepped) and the other at euglycemia (4.5 ± 0.1 mM) for 3 h and at a glucose level of 14.5 ± 0.3 mM for the subsequent 2 h (stepped). At comparable prevailing insulin concentrations, the rates of glucose uptake during the last 40 min of each 5-h study were 151 ± 7 and 154 ± 17 $\mu mol \cdot kg^{-1} \cdot min^{-1}$ during nonstepped and stepped studies, respectively (NS). Thus, when insulin action is allowed to be fully expressed (i.e., after ~3 h of insulin infusion), rates of glucose uptake are similar at a given prevailing glucose concentration regardless of how that glucose level is achieved, thus validating our experimental design.

The leg glucose-balance technique was performed as follows. Catheters were inserted into the femoral artery and vein with the modified Seldinger technique, and leg venous blood flow was measured by thermodilution, as previously validated (26,27) and described (21). Leg glucose uptake was calculated by the Fick principle (28) as the product of the arteriovenous glucose difference ($A\text{-}V_G$) and leg blood flow; blood glucose = plasma glucose × [1 − (0.3 × Hct)] (18).

Measurements of blood flow (5 determinations) were performed at the beginning and end of the euglycemic and hyperglycemic plateaus. The mean of 10 flow measurements at each glycemic plateau was taken as the representative value. The hematocrit was determined at each glycemic plateau.

Rates of glucose appearance (R_a) and disappearance (R_d) were measured in the basal state and during each of the NIMGU clamp studies by infusion of [3-^{3}H]glucose in a primed continuous manner. With this technique, 60 μCi of tracer was injected as a bolus dose, followed by a continuous infusion at a rate of 0.60 μCi/min. The tracer was allowed to label the glucose pool for 120 min, and glucose specific activity was measured for the subsequent 20 min at 5- to 10-min intervals. R_a and R_d were calculated with the Steele equations (29) assuming steady-state conditions. During the clamp studies (NIMGU studies only), blood samples were obtained at 10-min intervals to determine serum glucose concentration and plasma specific activity. R_a and R_d were calculated with the Steele equations in their modified derivative form, because the tracer exhibits non-steady-state kinetics under these conditions (30). We assumed a pool fraction of 0.65. Because the studies were performed at a serum glucose level above ~11 mM, the values for R_d were corrected for urinary glucose loss to reflect the actual rate of endogenous glucose disposal.

The isotope-dilution technique has been criticized because it tends to underestimate glucose R_a and thus R_d. Although the reasons for this have not been resolved (modeling error versus isotope impurity or both), the underestimate of R_a is greatest at high turnover rates in non–steady-state conditions. Turnover rates during insulinopenia are low and were measured under virtual steady-state conditions and therefore are not likely to be greatly affected by modeling error. The tracer was >99% pure and all from the same lot. Furthermore, we recently showed no difference in arteriovenous glucose specific activity with [3-^{3}H]glucose across the leg at high glucose turnover rates (31); therefore, it is unlikely that a tracer impurity existed.

For serum glucose determinations, blood was drawn, put in untreated polypropylene tubes, and centrifuged with an Eppendorf microcentrifuge (Brinkman, Westbury, NY). The glucose concentration of the supernatant was then measured by the glucose oxidase method with a glucose analyzer (YSI, Yellow Springs, OH). Blood for determination of serum insulin levels and plasma glucose specific activity was collected in untreated and treated tubes, respectively. The

specimens were spun, and the supernatant was removed and stored at −20°C. Serum insulin levels were measured by double-antibody radioimmunoassay (34); the lower detection limit of the insulin assay was 29 pM. All values reported as <29 pM were treated as representing 29 pM. Blood for determination of plasma C-peptide levels was collected in tubes containing EDTA and aprotinin (500 KIU/ml) and chilled, and the plasma was separated and frozen. C-peptide was measured by radioimmunoassay (35), and plasma FFA levels were measured by the method of Itaya and Vi (36). Plasma epinephrine levels were assayed by the isotope-derivative method (37).

All calculations and analyses were performed with the CLINFO data-base management and analysis program (Bolt, Beranek, and Newman, Cambridge, MA) operational at the University of California, San Diego, General Clinical Research Center. The data are presented as means ± SE unless otherwise indicated. Statistical analysis was done with Student's two-tailed *t* test for paired and unpaired data as indicated. The kinetic analysis of the data was performed by curve fitting (Fit Function routine, RS/1, BBN, Software Products, Cambridge, MA). This program performs a least-squares fit to the data. The data were assumed to follow the Michaelis-Menten equation $V = V_{max} \times [G]/(K_m + [G])$, where V is whole-body glucose uptake, leg glucose uptake, or A-V_G; $[G]$ is plasma glucose concentration; V_{max} is response at an infinite glucose concentration; and K_m is glucose concentration at half-maximum response. The only assumption in the analysis was that $V = 0$ at 0 glucose. At least five iterations were performed, and a value of 0.001 was used for convergence criterion to determine when to stop the fitting process. The unweighted group means of V and $[G]$ were used in the analysis. The RS/1 program assesses the validity of the fitted curve by analysis of variance. If the P value of the F statistic was <0.01, the fitted curve was assumed to fit the Michaelis-Menten equation. The estimates for K_m and V_{max} were defined to be accurate if the P values for the estimates (the final value of the estimate divided by its SE) was <0.20.

RESULTS

HORMONE AND METABOLIC DATA

NIMGU studies. The basal serum glucose level was 5.3 ± 0.1 mM. During SRIF-induced insulinopenia, the glucose level was clamped during each plateau period at 4.9 ± 0.1, 9.2 ± 0.2, 11.9 ± 0.3, and 20.5 ± 0.2 mM, respectively, with a coefficient of variation of <4% for all glucose plateaus. The basal serum insulin level was 45 ± 7 pM and fell during SRIF infusion to below detection limits of the assay (<29 pM, Fig. 2*A*, lower curve). Similarly, the basal C-peptide concentration was 360 ± 40 pM and was suppressed during SRIF infusion by ~85% of the basal value to steady-state levels of 37 ± 2, 29 ± 2, 30 ± 3, and 59 ± 7 pM at glucose plateaus of 4.9, 9.2, 11.9, and 20.5 mM, respectively (Fig. 2*B*). FFA levels rose from 0.115 ± 0.008 g/L in the basal state to 0.215 ± 0.021, 0.217 ± 0.021, 0.200 ± 0.015, and 0.207 ± 0.013 g/L during SRIF-induced insulinopenia at each respective glucose plateau ($P < 0.01$ basal vs. all other values). Thus, SRIF induced a profound and sustained state of insulin deficiency in the peripheral circulation throughout the NIMGU studies.

The basal epinephrine level was 370 ± 103 pM and during SRIF-induced insulinopenia was unchanged at each respective glucose plateau (220 ± 22, 210 ± 16, 170 ± 16, and 280 ± 71 pM, NS between all values).

IMGU studies. During insulin infusion, the glucose level was clamped sequentially at plateaus of 4.5 ± 0.1, 8.7 ± 0.1, 12.1 ± 0.5, and 21.0 ± 0.4 mM with a coefficient of variation of <4% for all glucose plateaus. Basal measurements were not obtained during the IMGU studies. During insulin infusion (40 mU · m^{-2} · min^{-1}), the serum insulin level remained constant throughout all glucose plateaus (502 ± 29, 466 ± 29, 496 ± 21, and 409 ± 57 pM, respectively, NS between all values; Fig. 2*A*), and the C-peptide levels were suppressed to a similar degree as in the NIMGU studies (Fig. 2*B*). During insulin infusion, the FFA levels were suppressed by 85% of the basal value.

The epinephrine levels remained unchanged throughout the period of insulin infusion at each respective glucose plateau (260 ± 16, 207 ± 38, 260 ± 49, and 210 ± 16 pM; NS between all values). In addition, the epinephrine levels throughout the IMGU studies were not different from those obtained during the NIMGU studies (NS between all values).

WHOLE-BODY GLUCOSE UPTAKE

NIMGU studies. During SRIF-induced insulinopenia, the rate of whole-body glucose uptake fell from a basal value of 11.2 ± 0.5 to 9.4 ± 0.3 μmol · kg^{-1} · min^{-1} at the first glucose plateau of 4.9 mM and subsequently increased to 14.0 ± 0.8, 16.2 ± 0.4, and 22.3 ± 2.4 μmol · kg^{-1} · min^{-1} at glucose plateaus of 9.2, 11.9, and 20.5 mM, respectively ($P < 0.05$ between any 2 consecutive values; Fig. 3). Corresponding

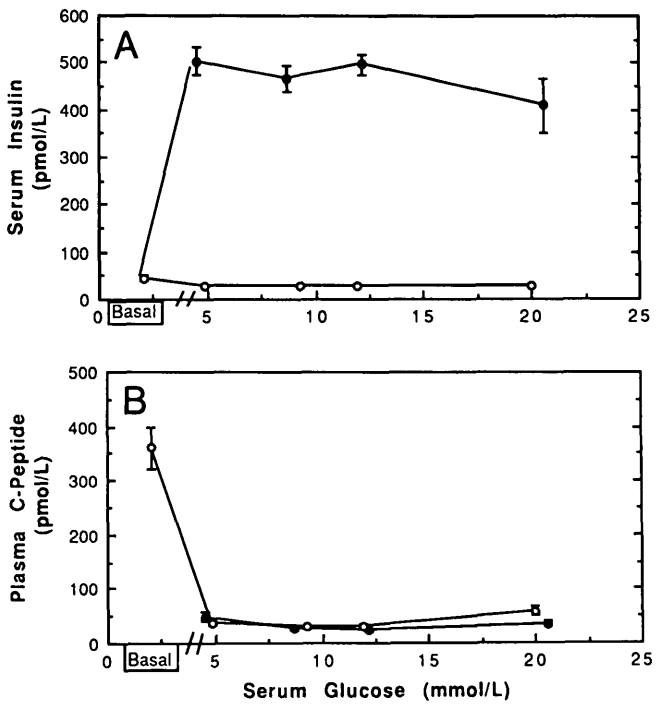

FIG. 2. Serum insulin (*A*) and C-peptide (*B*) levels during somatostatin infusion and constant insulin infusion of 40 mU · m^{-2} · min^{-1} (insulin-mediated glucose uptake; ●) or saline and somatostatin infusions (non–insulin-mediated glucose uptake; ○) at glucose concentrations of ~5, 9, 12, and 21 mM. Detection limit of insulin assay was 29 pM. Values are means ± SE.

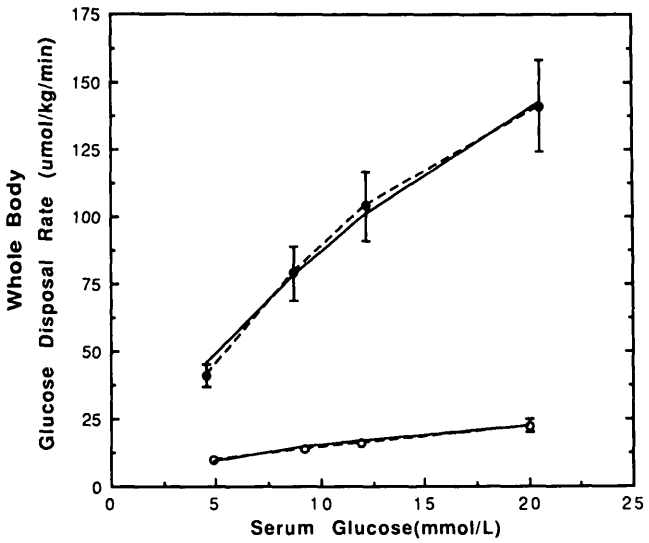

FIG. 3. Whole-body glucose uptake as function of prevailing serum glucose concentration. Whole-body rates of insulin-mediated glucose uptake (IMGU; ●) and non–insulin-mediated glucose uptake (NIMGU; ○) were measured at glucose concentrations of ~5, 9, 12, and 21 mM. IMGU = glucose disposal rate − NIMGU. *Solid lines* depict fit based on Michaelis-Menten equation. Values are means ± SE.

whole-body NIMGU rates (μmol/min) were 810 ± 33 (basal value), 677 ± 28, 960 ± 50, 1110 ± 39, and 1532 ± 166, respectively. The basal rate of hepatic glucose output was 11.6 ± 0.11 mM · kg^{-1} · min^{-1}, and fell during hypoinsulinemia to 8.1 ± 0.5, 5.0 ± 1.5, 3.8 ± 1, and −7.8 ± 2 μmol · kg^{-1} · min^{-1} at each successive glycemic plateau.

IMGU studies. Overall, whole-body GDRs increased threefold in a curvilinear fashion throughout the range of glucose studied from 50 ± 5 μmol · kg^{-1} · min^{-1} at the first glucose plateau of 4.5 mM to 93 ± 10, 121 ± 12, and 163 ± 16 μmol · kg^{-1} · min^{-1} at glucose plateaus of 8.7, 12.1, and 21.0 mM, respectively ($P < 0.01$ between any 2 consecutive values; Fig. 3). Corresponding whole-body GDRs were 3441 ± 350, 6363 ± 627, 8254 ± 815, and 11,152 ± 1104 μmol/min, respectively. Because GDR includes a non–insulin-mediated component, the NIMGU component was subtracted from the GDR at each glycemic plateau to obtain true rates of IMGU; i.e., IMGU = GDR − NIMGU. The rates of IMGU closely paralleled the GDR over the range of glucose studied (41 ± 4, 79 ± 10, 104 ± 13, and 141 ± 17 μmol · kg^{-1} · min^{-1} or 2764 ± 322, 5401 ± 655, 7150 ± 838, and 9625 ± 1121 μmol/min at each respective glucose plateau; $P < 0.01$ between any 2 consecutive values; Fig. 3).

Kinetic analysis. Curve fitting the data for whole-body glucose uptake resulted in an apparent V_{max} of 40 ± 5 and 359 ± 59 μmol · kg^{-1} · min^{-1} in the absence and presence of insulin, respectively. Thus, insulin increased the apparent V_{max} for whole-body glucose uptake approximately ninefold. The apparent K_m values were estimated at 17 ± 4 and 31 ± 7 mM for whole-body NIMGU and IMGU, respectively.

LEG GLUCOSE UPTAKE

NIMGU studies. The basal A-V_G across the leg was 0.12 ± 0.02 mM and fell during SRIF-induced insulinopenia to 0.09 ± 0.02 mM at the first glucose plateau of 4.9 mM and subsequently increased to 0.28 ± 0.03, 0.38 ± 0.05, and 0.59 ± 0.03 mM at glucose plateaus of 9.2, 11.9, and 20.5 mM, respectively ($P < 0.05$ between any 2 consecutive values excluding the basal measurement; Fig. 4*A*). Basal blood flow was 4.15 ± 0.63 dl/min and remained unchanged during SRIF infusion at each respective glucose plateau (Fig. 4*B*). Basal leg glucose uptake was 52 ± 15 μmol · min^{-1} · leg^{-1} and fell during SRIF-induced insulinopenia to 36 ± 9 μmol · min^{-1} · leg^{-1} at the first glucose plateau of 4.9 mM and subsequently increased in a near-linear fashion to 118 ± 15, 156 ± 17, and 260 ± 34 μmol · min^{-1} · leg^{-1} at each subsequent glucose plateau ($P < 0.05$ between any 2 consecutive values; Fig 4C).

IMGU studies. During insulin infusion, the A-V_G increased through the first three glucose plateaus (1.22 ± 0.11, 2.42 ± 0.26, and 3.00 ± 0.36 mM, respectively; $P < 0.01$ between each value) and did not significantly increase at the fourth and highest glycemic plateau (3.31 ± 0.36 mM, NS vs. the value at the 3rd glucose plateau). The NIMGU component was subtracted from the overall A-V_G during insulin infusion to obtain the A-V_G due only to insulin stimulation. The insulin-mediated A-V_G increased through the first three glucose plateaus but did not increase further despite the fact that the prevailing serum glucose concentration was raised to 21 mM at the highest glycemic plateau (Fig. 4*A*). In marked contrast to the results seen under insulinopenic conditions, during insulin infusion, leg blood flow increased twofold in a near-linear fashion over the range of glucose concentrations studied (from 6.0 ± 1.7 to 11.7 ± 3.1 dl/min, $P < 0.01$; Fig. 4*B*). Leg blood flow was higher during insulin infusion versus insulinopenia at the third and fourth glycemic plateaus only ($P < 0.05$). During insulin infusion, leg glucose uptake increased at every glucose plateau in a curvilinear fashion (774 ± 270, 1543 ± 545, 2451 ± 610, and 3656 ± 931 μmol · min^{-1} · leg^{-1}; $P < 0.05$ between any 2 consecutive values). Because rates of leg NIMGU are relatively small, the rates of leg IMGU (IMGU = GDR − NIMGU) closely paralleled the rates of overall leg glucose disposal (Fig. 4*C*). This curvilinear increase in leg IMGU is similar to the whole-body IMGU curve (Fig. 3).

Kinetic analysis. Although the data for leg glucose uptake fit the Michaelis-Menten equation, the estimates of K_m and V_{max} were inaccurate due to the large error observed and better fit a linear function.

IMGU is a function of the serum insulin concentration, the prevailing serum glucose concentration, and blood flow (glucose delivery) to tissues. Changes in blood flow were observed over the range of glucose concentrations in the presence of insulin and thus confound the kinetic analysis of tissue glucose uptake. Therefore, the effect of glucose concentration on IMGU, independent of blood flow, is more accurately represented by the A-V_G (or glucose extraction) across the leg than by leg glucose uptake (which includes the component of leg blood flow). The A-V_G data were fitted to the Michaelis-Menten equation, and this analysis resulted in a good fit for the A-V_G data obtained during insulin infusion with a V_{max} of 4.2 ± 1 mM and an apparent K_m of 9.1 ± 6 mM. In contrast, although the A-V_G data obtained in the absence of insulin fit Michaelis-Menten kinetics, the estimates of the kinetic parameters ($K_m > 200$ mM and V_{max} near infinity) were highly inaccurate due to the large error observed. These data were found to better fit a linear function. There-

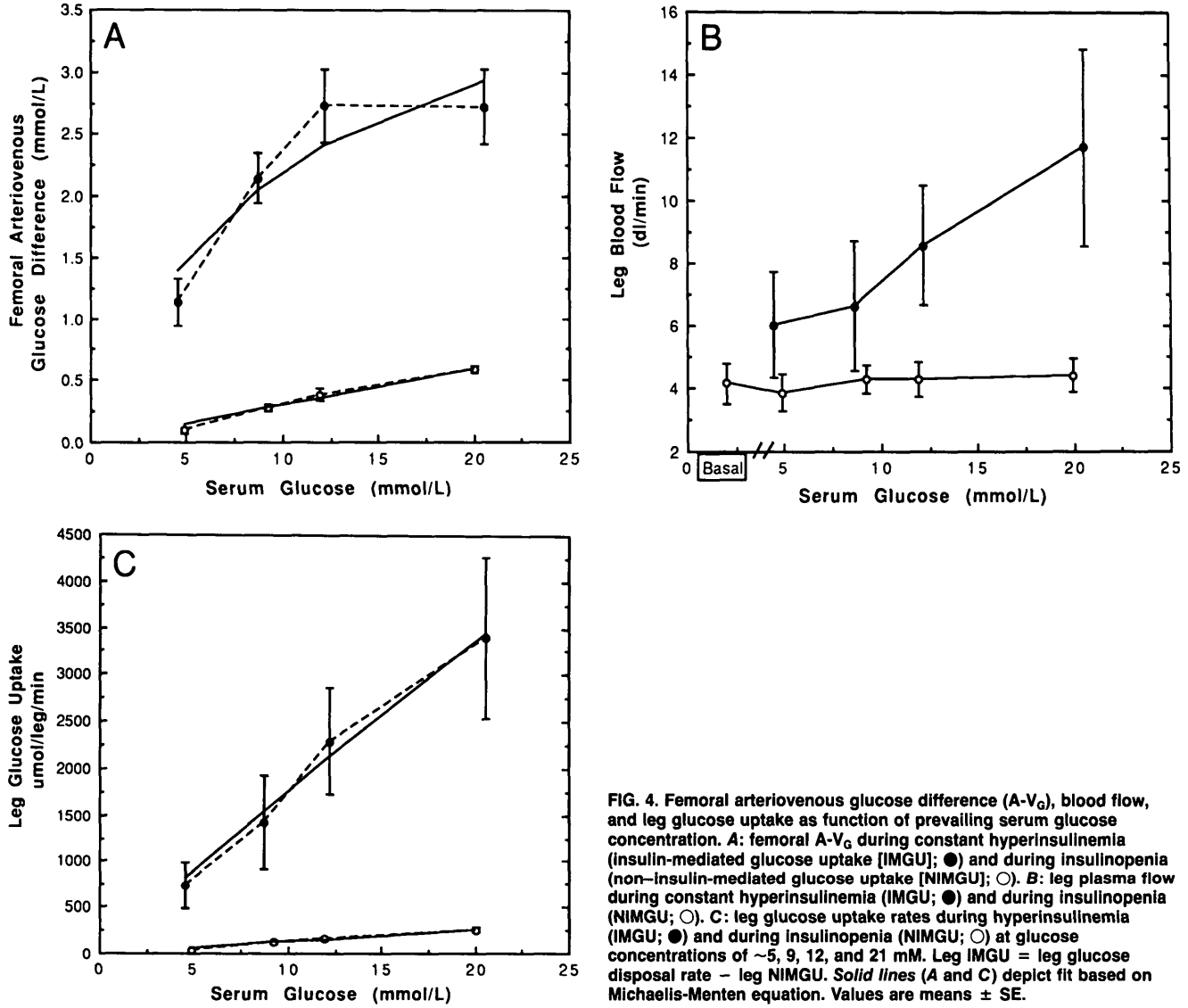

FIG. 4. Femoral arteriovenous glucose difference (A-V_G), blood flow, and leg glucose uptake as function of prevailing serum glucose concentration. *A*: femoral A-V_G during constant hyperinsulinemia (insulin-mediated glucose uptake [IMGU]; ●) and during insulinopenia (non–insulin-mediated glucose uptake [NIMGU]; ○). *B*: leg plasma flow during constant hyperinsulinemia (IMGU; ●) and during insulinopenia (NIMGU; ○). *C*: leg glucose uptake rates during hyperinsulinemia (IMGU; ●) and during insulinopenia (NIMGU; ○) at glucose concentrations of ~5, 9, 12, and 21 mM. Leg IMGU = leg glucose disposal rate − leg NIMGU. *Solid lines* (*A* and *C*) depict fit based on Michaelis-Menten equation. Values are means ± SE.

fore, to better appreciate the kinetic parameters over the physiological range of serum glucose concentrations actually studied, we obtained the individual glucose concentrations at which one-half of the highest A-V_G was achieved, and these values were designated as the half-maximal effective glucose concentration (EG_{50}). The mean EG_{50} values for glucose extraction across leg muscle were 10.0 ± 0.4 and 5.3 ± 0.1 mM in the absence and presence of insulin, respectively ($P < 0.01$), and the maximal A-V_G values (obtained at ~20 mM glucose) were 0.59 ± 0.03 and 2.72 ± 0.3 mM, respectively. Therefore, it is apparent that insulin increased the capacity approximately fivefold and the affinity approximately twofold of muscle glucose extraction over the range of glucose concentrations studied.

DISCUSSION

This study was performed to examine the effect of insulin on the capacity and affinity of in vivo glucose uptake in skeletal muscle. The results indicate an effect of insulin to increase both the capacity and affinity of muscle glucose uptake.

Relatively few studies have examined the kinetics of in vivo glucose uptake in humans. Gottesman et al. (17) studied whole-body insulin-stimulated GDRs and interpreted their data on the basis of the glucose-transport model as suggested by Cushman et al. (38) and Suzuki et al. (39). They found an increase in V_{max} without a change in K_m and concluded that insulin stimulates glucose uptake by increasing the number of glucose-transport sites on the plasma membrane and that these transport sites have the same affinity for glucose as those present in the basal state. However, during these studies, glucose uptake was measured over a relatively narrow range of serum glucose concentrations (3.3–8.9 mM) over which saturation of the glucose-uptake system was not approached; therefore, the K_m could not be ascertained. Fink et al. (40) measured rates of whole-body glucose uptake over a wide range of glucose concentrations during constant hyperinsulinemia (~718 pM) and determined that whole-body glucose uptake did not follow Michaelis-Menten kinetics. There are several possible reasons for this. *1*) Whole-body glucose uptake represents a composite of various individual tissues that likely display different kinetic (K_m/V_{max}) characteristics (41–43). *2*) In vivo glucose uptake occurs via two distinct mechanisms, i.e., IMGU, which occurs by definition only in insulin-sensitive tissues,

and NIMGU, which occurs in insulin-sensitive and insulin-insensitive tissues (19,20,44). Although at euglycemia, most NIMGU occurs in the central nervous system (45–48), at higher glucose concentrations, an increasing proportion of NIMGU occurs, by a mass action effect, in non–central nervous system tissues. This is evident from our data demonstrating a significant rise in leg NIMGU as glucose concentration was increased (Fig. 4*C*). To specifically analyze the IMGU system, the NIMGU component should be factored out; NIMGU was not directly measured during previous kinetic studies (17,18,40). *3*) As shown by our results, blood flow can change at different levels of IMGU, confounding the kinetic analysis of tissue glucose uptake per se.

Yki-Järvinen et al. (18) carried out forearm-balance studies to examine the kinetics of insulin-stimulated glucose disposal in skeletal muscle. Their findings in forearm skeletal muscle mirrored their findings for the whole body, i.e., at higher insulin concentrations, insulin-stimulated glucose disposal did not saturate over the range of glucose concentrations studied. Similarly, we noted that, during insulin stimulation, leg muscle and whole-body glucose disposal rates did not saturate over the range of glucose concentrations studied. The similarity of these findings, however, is not as straightforward as it appears. Yki-Järvinen et al. reported no significant change in forearm blood flow measured by capacitance plethysmography during insulin and glucose infusions, suggesting that A-V_G markedly increased at all glucose concentrations, because forearm glucose uptake (A-V_G × flow) did not saturate. In contrast, we observed a linear increase in leg blood flow with increments in the prevailing serum glucose concentration during constant hyperinsulinemia (Fig. 4*B*) and noted saturation of glucose extraction as determined by the lack of change in A-V_G between glucose concentrations of 12.1 and 21.0 mM (Fig. 4*A*). Because A-V_G was unchanged, it follows that the increment in leg blood flow between glucose concentrations of 12.1 and 21.0 mM was responsible for the significant increase in leg glucose uptake between these two glucose concentrations. Therefore, the increment in blood flow was responsible for the apparent lack of saturation of in vivo leg glucose uptake.

The differences between our findings and those of Yki-Järvinen could be the result of different experimental techniques. Although the forearm-balance technique, as used in their study, has yielded valuable data, it has several drawbacks: *1*) The forearm drains in a venous plexus (49), making it difficult to ensure the reproducibility of venous sampling during studies requiring repeated catheterizations; *2*) measurement of forearm blood flow requires the exclusion of hand flow, which can modulate the distribution of forearm flow and venous drainage (50); *3*) heating the hand to obtain arterialized venous blood results in redistribution of blood flow in the contralateral forearm, which can lead to erroneous A-V_G data and flow measurements (51).

We found a highly significant correlation between leg blood flow rates and rates of whole-body IMGU ($r = 0.55$, $P < 0.005$), suggesting that leg blood flow reflects blood flow to other body muscle beds and is an important determinant of overall rates of IMGU in the whole body. At first glance, we might infer that this increment in flow impacts on the kinetic characteristics of tissue glucose extraction (A-V_G). This, however, is not the case. For an increase in flow to decrease A-V_G, it must decrease the mean intravascular transit time ($\bar{t}_{vasc}$) for glucose through the limb (28). That is, the time a glucose molecule spends in the capillary must decrease, or the velocity of a glucose molecule through the capillary network must increase. Furthermore, the decrease in $\bar{t}_{vasc}$ must approach the diffusion time for glucose to go from the intravascular space to the intercellular space (~0.1 s; 52). Recent data from our laboratory (this issue, p. 965) indicate that the $\bar{t}_{vasc}$ for glucose was unchanged at low and high flow rates (~1.4 s). The $\bar{t}_{vasc}$ is equal to the intravascular volume of distribution (V_d) of glucose in the leg divided by the blood flow ($\bar{t}_{vasc} = V_d$/blood flow; 53), and because we found no change in the $\bar{t}_{vasc}$ for glucose over the observed range of plasma flow, it follows that increases in leg blood flow during insulin stimulation were accompanied by corresponding increases in the intravascular volume of distribution of glucose. These data are in agreement with those of Ferrannini et al. (43), who also reported an effect of insulin to increase the volume of distribution of glucose. Overall, the results are consistent with the formulation that increases in the glucose volume of distribution represent recruitment of previously unperfused or underperfused capillary beds leading to increases in leg muscle mass available for IMGU. This increment in flow does not, however, alter A-V_G, because each increment in extraction capacity (tissue recruitment) is matched by a corresponding increase in glucose delivery (blood flow); i.e., V_d/blood flow remains constant. Therefore, to ascertain the V_{max} and K_m of tissue glucose uptake independent of changes in blood flow, we analyzed A-V_G (glucose extraction) across leg muscle.

The maximal capacity for leg muscle insulin-mediated glucose extraction was achieved at a glucose concentration of ~12 mM, indicating saturation of glucose-extraction mechanisms. In contrast, during insulin deficiency, A-V_G increased linearly at all glucose concentrations (Fig. 4*A*), suggesting no saturation of leg muscle NIMGU over the range of glucose concentrations studied. Nevertheless, by comparing the femoral A-V_G obtained at the highest glucose concentration in the absence and presence of insulin, it is apparent that insulin had the effect of increasing this value approximately fivefold. To compare the functional forms of the kinetic curves, we expressed the A-V_G at each glycemic plateau as a percentage of the maximal value (Fig. 5). By this analysis, the glucose concentration at which leg muscle glucose extraction was one-half of the maximal value (EG_{50}) was 5.3 ± 0.4 mM during insulin infusion and 10.0 ± 0.4 during insulinopenia ($P < 0.01$). Therefore, the NIMGU system is characterized by an EG_{50} for muscle glucose uptake that is at least twice as high as the EG_{50} for the IMGU system.

Because blood flow did not change during measurements of NIMGU, leg NIMGU or whole-body NIMGU can provide estimates of the tissue kinetic parameters. Note that, by this analysis, we found that the EG_{50} for whole-body NIMGU was significantly lower than that obtained for leg muscle NIMGU (6.2 ± 0.4 vs. 9.78 ± 0.90 mM, $P < 0.02$). Therefore, NIMGU in body tissues other than those participating in leg NIMGU are characterized as a whole by an EG_{50} markedly lower than the EG_{50} for leg NIMGU. This is consistent with the notion that the brain has a low K_m for glucose uptake, which has been estimated in dogs to be ~2 mM (54).

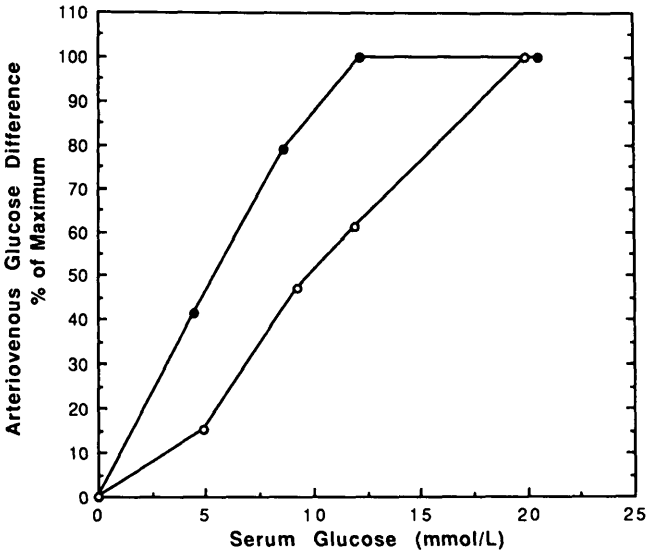

FIG. 5. Kinetics analysis of insulin-mediated (IMGU) and non–insulin-mediated (NIMGU) leg glucose uptake. Femoral arteriovenous glucose difference ($A\text{-}V_G$) is expressed as percentage of maximal $A\text{-}V_G$ as function of prevailing serum glucose concentrations during hyperinsulinemia (IMGU; ●) and insulinopenia (NIMGU; ○).

With respect to IMGU, it is interesting that extrapolation from leg to whole-body rates of skeletal muscle glucose uptake, in some cases, gave rise to estimates that exceeded whole-body glucose turnover rates. This is in contrast to our previous study, in which similar calculations were performed with plasma flow rates (~40% lower than rates of blood flow; 21). The reason for this is probably multifactorial and could be due to overestimation of leg muscle blood flow and/or glucose uptake, underestimation of whole-body glucose uptake, wrong assumptions about leg and body muscle mass, the distribution of cardiac output to various muscle groups, or the contribution of erythrocyte glucose to tissue glucose uptake.

Several reports have documented an effect of insulin to increase blood flow to skeletal muscle. Liang et al. (55), using the radioactive-microsphere method, demonstrated a 2.7-fold increase above basal level of skeletal muscle blood flow in dogs during euglycemic-hyperinsulinemic glucose-clamp studies. These authors also documented increased cardiac output and decreased peripheral vascular resistance in response to insulin. Note that both blood pressure and heart rate were unchanged from basal levels during any of our studies at all leg flow rates, also supporting an effect of insulin to decrease peripheral vascular resistance. Gelfand et al. (56), using the dye-dilution technique, and Creager et al. (57), using strain-gauge plethysmography, recently reported 25 and 50% increases, respectively, in forearm blood flow during an intrabrachial artery infusion of insulin without changes in arterial pressure. More recently, Richter et al. (58), using the thermodilution technique, described the effect of insulin given systemically to increase thigh blood flow in humans. We recently described an effect of insulin to increase leg blood flow ~2-fold from baseline in a dose-dependent fashion with an ED_{50} of ~250 pM in lean subjects (59). These data suggest a role for insulin to mediate increases in blood flow to skeletal muscle by increasing cardiac output and through peripheral vasodilation. Ours is the first report of an effect of the prevailing serum glucose concentration to modulate blood flow during hyperinsulinemia.

Note also that other investigators observed small but insignificant increases in leg blood flow rates with the dye-dilution technique (46). Other limb-balance studies with plethysmographic techniques to measure flow rates did not report an increase in blood flow rates during hyperinsulinemic glucose-clamp studies (18,60,61). The reasons for these discrepancies are not clear, but they are likely the result of the different techniques used.

To assess the impact of increases in blood flow on IMGU, we can calculate what leg glucose uptake would be if the blood flow were fixed by multiplying the $A\text{-}V_G$ obtained at each glycemic level by the blood flow rate obtained at the first glycemic plateau (4.1 dl/min). In this hypothetical situation, leg glucose uptake at the highest glycemic plateau would be ~50% lower than the actual value when leg blood flow was 11.7 dl/min. In support of a role for blood flow to modulate IMGU, Schultz et al. (62,63) showed that in the perfused rat hindlimb, glucose delivery (blood flow) is an important modulator and is directly correlated with glucose uptake. Previous studies of glucose uptake in vivo (1,17), including those from our group (2,40), ignored potential changes in blood flow to insulin-sensitive tissues and implicitly assumed that the flow component was fixed. Changes in blood flow may have important implications for the interpretation of tissue insulin sensitivity as assessed by measurements of rates of whole-body IMGU.

The most widely accepted model for cellular glucose transport suggests that, on insulin stimulation, intracellular glucose transporters are translocated to the plasma membrane where they are also activated, resulting in an increase in the V_{max} (38,39). If the rate-limiting step for in vivo glucose uptake is the glucose-transport system, our results, in accordance with this model, are most consistent with an effect of insulin to increase glucose uptake by increasing the number and/or activity of glucose transporters and by increasing the overall affinity of the transporters for glucose. NIMGU could represent a low-affinity glucose-uptake system in skeletal muscle, NIMGU into nonskeletal muscle tissues in the leg (e.g., endothelial cells, erythrocytes, neural tissue) via a low-affinity system, or both. Insulin's effect to decrease the apparent K_m for glucose uptake could occur by *1*) transforming the low-affinity NIMGU systems into a high-affinity IMGU system or *2*) making available a high-affinity IMGU system that functionally dominates the constitutive low-affinity NIMGU system. The finding by James et al. (64) of the presence of both insulin-stimulable and insulin-unstimulable glucose transporters within insulin target cells and data from our laboratory demonstrating that IMGU and NIMGU are separately regulated in vivo glucose-uptake systems supports this latter construct. Regardless of the cellular basis, the uptake system responsible for muscle NIMGU displays very different kinetic characteristics from those of the IMGU system. The IMGU system displays an EG_{50} (~5 mM) consistent with the K_m of the glucose-transport system as measured in vitro, supporting the view that glucose transport is rate limiting for in vivo glucose uptake during insulin stimulation at all glucose disposal rates.

ACKNOWLEDGMENTS

This work was supported in part by Grant AM-33649 from the National Institute of Diabetes and Digestive and Kidney Diseases, National Institutes of Health (NIH); Grant RR-00827 from the General Clinical Research Center Branch, NIH; the Juvenile Diabetes Foundation; and a grant from the Veterans Administration Research Service. A.D.B. was a Clinical Associate Physician of the General Clinical Research Center, NIH, and the recipient of a Juvenile Diabetes Foundation Research grant. S.V.E. was a Postdoctoral Fellow at the University of California, San Diego. M.L. was a visiting scientist from the University of Kuopio, Finland, and a recipient of International Research Fellowship Grant TW-03969-01, The Fogarty International Center, NIH.

We are deeply indebted to Drs. Maurice Buchbinder and Todd Sherman for expert assistance in inserting the femoral catheters. We also thank Cleon Tate and Erin Frew for invaluable secretarial assistance and the staff of the Special Diagnostic and Treatment Unit, Veterans Administration Hospital, San Diego, California, for supportive assistance. We also acknowledge Dr. K.S. Polonsky's laboratory, University of Chicago, for kindly performing the C-peptide radioimmunoassay (Diabetes Research Training Grant DK-20595).

REFERENCES

1. Rizza RA, Mandarino JL, Gerich JF: Dose response characteristics for effects of insulin on production and utilization in man. *Am J Physiol* 240:E630–39, 1981
2. Kolterman OG, Gray RS, Griffin J, Burstein P, Insel J, Scarlett JA, Olefsky JM: Receptor and postreceptor defects contribute to insulin resistance in non-insulin dependent diabetes mellitus. *J Clin Invest* 68:957–69, 1981
3. Campbell PJ, Mandarino LJ, Gerich JE: Quantification of the relative impairment in actions of insulin on hepatic glucose production and peripheral glucose uptake in non-insulin dependent diabetes mellitus. *Metabolism* 37:15–21, 1988
4. Ludvigsen D, Jarett L: A comparison of basal and insulin-stimulated glucose transport in rat adipocyte plasma membranes. *Diabetes* 29:373–78, 1980
5. Olefsky JM: Mechanisms of the ability of insulin to activate the glucose transport system in rat adipocytes. *Biochem J* 172:137–45, 1978
6. Whitesell R, Gliemann J: Kinetic parameters of transport of 3-O-methylglucose and glucose in adipocytes. *J Biol Chem* 254:5276–83, 1979
7. Wardzala L, Cushman S, Salans L: Mechanism of insulin action on glucose transport in the isolated rat adipose cell. *J Biol Chem* 253:8002–8005, 1978
8. Ciaraldi T, Kolterman O, Siegel J, Olefsky JM: Insulin-stimulated glucose transport in human adipocytes. *Am J Physiol* 236:E621–25, 1979
9. Czech M, Lawrence J, Lynn W: Hexose transport in isolated brown fat cells: a model system for investigating insulin action and membrane transport. *J Biol Chem* 249:5421–27, 1974
10. Morgan H, Regen D, Park C: Identification of a mobile carrier-mediated sugar transport system in muscle. *J Biol Chem* 239:369–74, 1964
11. Chandry I, Gould M: Kinetics of glucose uptake in isolated soleus muscle. *Biochim Biophys Acta* 177:527–36, 1969
12. Wardzala LJ, Jeanrenaud B: Potential mechanism of insulin action on glucose transport in the isolated rat diaphragm: apparent translocation of intracellular transport units to the plasma membrane. *J Biol Chem* 256:7090–93, 1981
13. Ploug T, Galbo H, Vinten J, Jorgensen M, Richter EA: Kinetics of glucose transport in rat muscle: effects of insulin and contractions. *Am J Physiol* 253:E12–20, 1987
14. Toyoda N, Flanagan JE, Kono T: Reassessment of insulin effects on the V_{max} and K_m values of hexose transport in isolated rat epididymal adipocytes. *J Biol Chem* 262:2737–45, 1987
15. Whitesell RR, Abumrad NA: Increased affinity predominates in insulin stimulation of glucose transport in the adipocyte. *J Biol Chem* 260:2894–99, 1985
16. Suzuki K: Reassessment of the translocation hypothesis by kinetic studies on hexose transport in isolated rat adipocytes. *J Biol Chem* 283:12247–51, 1988
17. Gottesman I, Mandarino L, Verdonk C, Rizza R, Gerich J: Insulin increases the maximum velocity for glucose uptake without altering the Michaelis constant in man. *J Clin Invest* 70:1310–14, 1982
18. Yki-Järvinen H, Young AA, Lamkin C, Foley JE: Kinetics of glucose disposal in whole body and across the forearm in man. *J Clin Invest* 79:1713–19, 1987
19. Baron AD, Wallace P, Brechtel G: In vivo regulation of non-insulin mediated and insulin mediated glucose uptake by epinephrine. *J Clin Endocrinol Metab* 64:889–95, 1987
20. Baron AD, Wallace P, Brechtel G: In vivo regulation of non-insulin-mediated and insulin-mediated glucose uptake by cortisol. *Diabetes* 36: 1230–37, 1987
21. Baron AD, Brechtel G, Wallace P, Edelman SV: Rates and tissue sites of non-insulin- and insulin-mediated glucose uptake in humans. *Am J Physiol* 255:E769–74, 1988
22. National Diabetes Data Group: Classification and diagnosis of diabetes mellitus and other categories of glucose intolerance. *Diabetes* 28:1039–57, 1979
23. Gray RS, Scarlett JA, Griffin J, Olefsky JM, Kolterman OG: In vivo deactivation of peripheral, hepatic, and pancreatic insulin action in man. *Diabetes* 31:929–36, 1982
24. Prager R, Wallace P, Olefsky JM: In vivo kinetics of insulin action on peripheral glucose disposal and hepatic glucose output in normal and obese subjects. *J Clin Invest* 78:472–81, 1986
25. Baron AD, Wallace P, Brechtel G, Prager R: Somatostatin does not increase insulin-stimulated glucose uptake in humans. *Diabetes* 36:33–36, 1987
26. Fronek A, Ganz V: Measurement of flow in single blood vessels including cardiac output by local thermodilution. *Circ Res* 8:178–83, 1960
27. Ganz V, Hlavova A, Fronek A, Luihard J, Prerovsky I: Measurement of blood flow in the femoral artery in man at rest and during exercise by local thermodilution. *Circulation* 30:86–89, 1964
28. Zierler KL: Theory of the use of arteriovenous concentration differences for measuring metabolism in steady and non-steady state. *J Clin Invest* 40:2111–25, 1961
29. Steele R: Influence of glucose loading and injected insulin on hepatic glucose output. *Ann NY Acad Sci* 82:420–30, 1959
30. Chiasson JL, Liljenquist JE, Lacy WW, Jennings AS, Cherrington AD: Gluconeogenesis: methodological approaches in vivo. *Fed Proc* 36:229–35, 1977
31. Molina JM, Baron AD, Edelman SV, Olefsky JM: Variable tracer infusion rate improves determination of glucose turnover in man. *Am J Physiol* 258:E16–23, 1990
34. Desbuquois B, Aurbach GD: Use of polyethylene glycol to separate free and antibody bound peptide hormones in radioimmunoassays. *J Clin Endocrinol Metab* 33:732–38, 1971
35. Kuzuya H, Blix PM, Horwitz DL, Steiner DF, Rubenstein AH: Determination of free and total insulin and C-peptide in insulin-treated diabetes. *Diabetes* 26:22–29, 1977
36. Itaya K, Vi M: Colorimetric determination of free fatty acids in biological fluids. *J Lipid Res* 6:16–20, 1965
37 Cryer P, Santiago J, Shah S: Measurement of norepinephrine and epinephrine in small volumes of human plasma by a single isotope derivative method: response to upright posture. *J Clin Endocrinol Metab* 39:1025, 1974
38. Cushman S, Wardzala L: Potential mechanism of insulin action on glucose transport in the isolated rat adipose cell: apparent translocation of intracellular transport systems to the plasma membrane. *J Biol Chem* 255:4728–62, 1980
39. Suzuki K, Kono T: Evidence that insulin causes translocation of glucose transport activity to the plasma membrane from an intracellular storage site. *Proc Natl Acad Sci USA* 77:2542–45, 1980
40. Fink RI, Wallace P, Olefsky JM: Effects of aging on glucose-mediated glucose disposal and glucose transport. *J Clin Invest* 77:2034–41, 1986
41. Kraegen EW, James DE, Jenkins AB, Chisolm DJ: Dose-response curve for in vivo insulin sensitivity in individual tissues in rat. *Am J Physiol* 248:E353–62, 1985
42. DeFronzo RA, Ferrannini E, Hendler R, Felig P, Wahren J: Regulation of splanchnic and peripheral glucose uptake by insulin and hyperglycemia in man. *Diabetes* 32:35–45, 1983
43. Ferrannini E, Smith JD, Cobelli C, Toffolo G, Pilo A, DeFronzo RA: Effect of insulin on the distribution and disposition of glucose in man. *J Clin Invest* 76:357–64, 1985
44. Baron AD, Kolterman OG, Bell J, Mandarino LJ, Olefsky JM: Rates of non-insulin-mediated glucose uptake are elevated in type II diabetic subjects. *J Clin Invest* 76:1782–88, 1985
45. DeFronzo RA, Jacot E, Jequier E, Maeder E, Wahren J, Felber JP: The effect of insulin on the disposal of intravenous glucose: results from indirect calorimetry and hepatic and femoral venous catheterization. *Diabetes* 30:1000–1007, 1981
46. DeFronzo RA, Ferrannini E, Sato Y, Felig P, Wahren J: Synergistic interaction between exercise and insulin on peripheral glucose uptake. *J Clin Invest* 68:1468–74, 1981
47. Scheinberg FP: Observation on cerebral carbohydrate metabolism in man. *Ann Intern Med* 62:367–71, 1965
48. Huang SC, Phelps ME, Hoffman EJ, Sideris K, Selin CJ, Kuhl KE: Noninvasive determination of local cerebral metabolic rate of glucose in man. *Am J Physiol* 238:E69–82, 1980

49. Coles DR, Cooper KE, Mottram RF, Occleshaw JV: The source of blood samples withdrawn from deep forearm veins via catheters passed upstream from the median cubital vein. *J Physiol* (Lond) 142:323–28, 1958
50. Levenson J, Simon A, Pithois-Merli I: Brachial arterial changes in response to wrist occlusion in normotensive and hypertensive men. *Am J Physiol* 253:H217–24, 1987
51. Astrup A, Simonsen L, Bulow J, Christensen NJ: Measurement of forearm oxygen consumption: role of heating the contralateral hand. *Am J Physiol* 255:E572–78, 1988
52. Bassingthwaighte JB: Overview of the processes of delivery: flow, transmembrane transport, reaction, and retention. *Circulation* 72 (Suppl. 4): 39–46, 1985
53. Bassingthwaighte JB, Holloway GA: Estimation of blood flow with radioactive tracers. *Semin Nucl Med* 6:141–61, 1976
54. Lund-Andersen H: Transport of glucose from blood to brain. *Physiol Rev* 59:305–51, 1979
55. Liang CS, Doherty JU, Faillace R, Maekawa K, Arnold S, Gavras H, Hood WB Jr: Insulin infusion in conscious dogs: effects on systemic and coronary hemodynamics, regional blood flows, and plasma catecholamines. *J Clin Invest* 69:1321–28, 1982
56. Gelfand RA, Barrett EJ: Effect of physiologic hyperinsulinemia on skeletal muscle protein synthesis and breakdown in man. *J Clin Invest* 80:1–6, 1987
57. Creager MA, Liang CS, Coffman JD: Beta adrenergic-mediated vasodilator response to insulin in the human forearm. *J Pharmacol Exp Ther* 235:709–14, 1985
58. Richter EA, Mikines KJ, Galbo H, Kiens B: Effect of exercise on insulin action in human skeletal muscle. *J Appl Physiol* 66:876–85, 1989
59. Laakso M, Edelman SV, Brechtel G, Baron AD: Decreased effect of insulin to stimulate skeletal muscle blood flow in obese man: a novel mechanism for insulin resistance. *J Clin Invest*. In press
60. Jackson RA, Roshania RD, Hawa MI, Sim BM, DiSilvio L: Impact of glucose ingestion on hepatic and peripheral glucose metabolism in man: an analysis based on simultaneous use of the forearm and double isotope techniques. *J Clin Endocrinol Metab* 63:541–49, 1986
61. Jackson RA, Hamling JB, Blix PM, Sim BM, Hawa MI, Jaspan JB, Belin J, Navarro JDN: The influence of graded hyperglycemia with and without physiological hyperinsulinemia on forearm glucose uptake and other metabolic responses in man. *J Clin Endocrinol Metab* 63:594–603, 1986
62. Schultz TA, Lewis SB, Westbie DK, Gerich JE, Rushakoff RJ, Wallin JD: Glucose delivery—a clarification of its role in regulating glucose uptake in rat skeletal muscle. *Life Sci* 20:733–36, 1977
63. Schultz TA, Lewis SB, Westbie DK, Wallin JD, Gerich JE: Glucose delivery: a modulator of glucose uptake in contracting skeletal muscle. *Am J Physiol* 223:E514–18, 1977
64. James DE, Brown R, Navarro J, Pilch PF: Insulin-regulatable tissues express a unique insulin-sensitive glucose transport protein. *Nature* (Lond) 333:183–85, 1988